


Assessing the potential impacts of climate change on streamflow in the data-scarce Upper Ruvu River watershed, Tanzania

Nickson Tibangayuka ^{*}, Deogratias M. M. Mulungu  and Fides Izdori

Department of Water Resources Engineering, University of Dar es Salaam, P.O. Box 35131, Dar es Salaam, Tanzania

*Corresponding author. E-mail: nicktib@outlook.com

 NT, 0000-0002-3207-4632; DMMM, 0000-0003-2283-9918

ABSTRACT

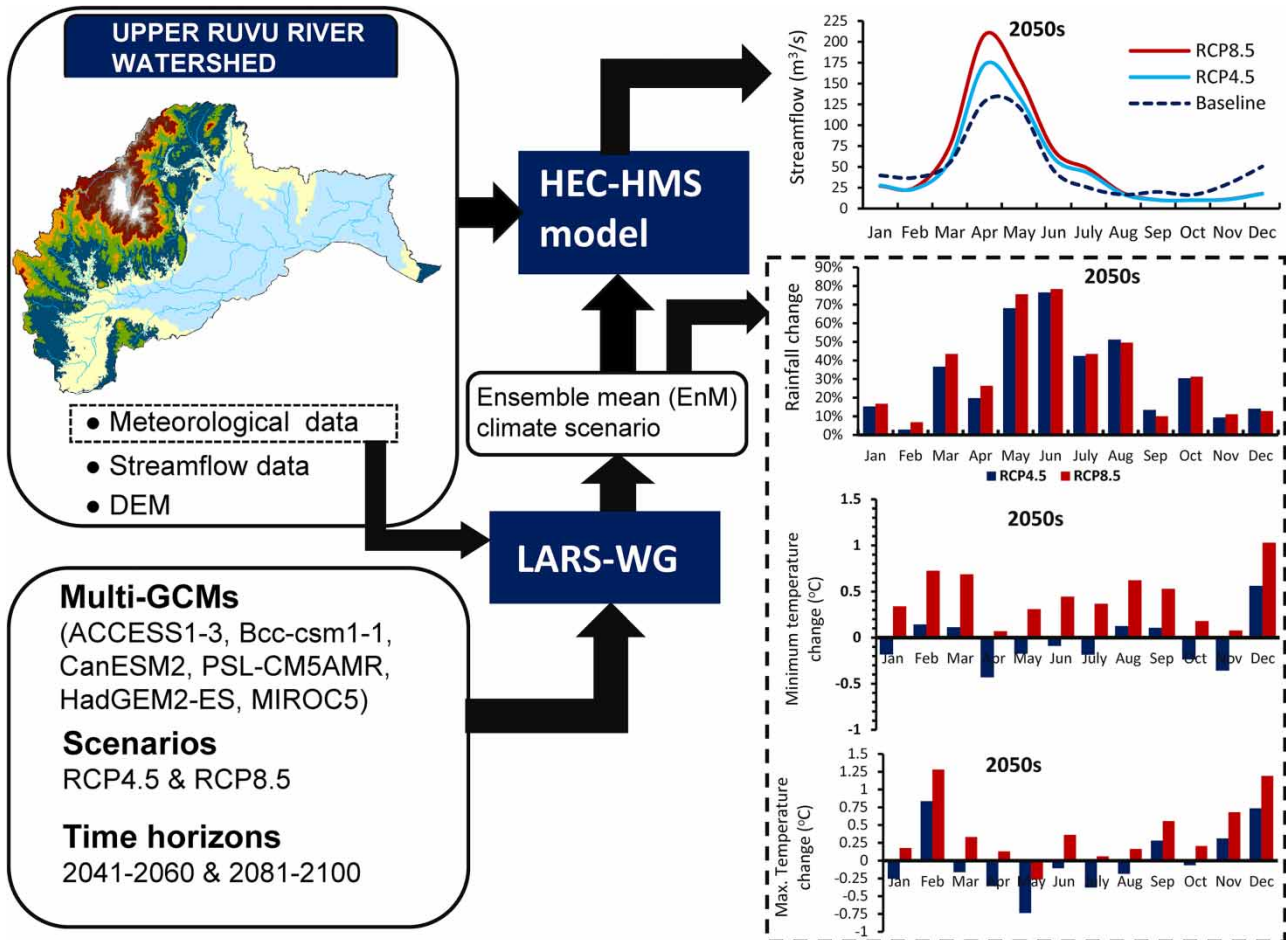
This study assessed the impacts of climate change on streamflow in the data-scarce Upper Ruvu River watershed (URRW). The Long Ashton Research Station Weather Generator (LARS-WG) was employed for generating the future ensemble-mean climate scenario based on six global circulation models (GCMs), under two representative concentration pathways (RCPs: RCP4.5 and RCP8.5). The future projections were made in two periods (2041–2060 and 2081–2100), and the baseline period (1951–1978) was used as a reference. The watershed hydrology was represented by the Hydrologic Engineering Center's Hydrologic Modeling System (HEC-HMS) model, which was calibrated and validated by using 5 and 4 years of streamflow data, respectively. Results indicate that the rainfall and minimum and maximum temperatures will increase in both periods, under both scenarios. This will potentially affect the streamflow that is projected to increase from March to August and decrease from September to February. The mean annual streamflow could potentially change from 48 m³/s in the baseline period to 45.6 and 56.5 m³/s during 2041–2060, and 52.4 and 67.4 m³/s during 2081–2100, under RCP4.5 and RCP8.5, respectively. The minimum and maximum streamflows are also predicted to change in both periods, under both scenarios. Considering these results, the climate change will have significant impacts on the streamflows of the URRW.

Key words: climate change, HEC-HMS, multi-GCMs, RCPs, streamflow, Upper Ruvu River watershed

HIGHLIGHTS

- The climate change impacts on streamflow were assessed in two future periods (2050s and 2080s) under RCP4.5 and RCP8.5.
- The rainfall and temperature are projected to increase in both periods under RCP4.5 and RCP8.5.
- The climate change will have significant impacts on the streamflow of the Upper Ruvu River watershed.

GRAPHICAL ABSTRACT



INTRODUCTION

Climate change is one of the most delicate subjects in many catchments around the world (Niang *et al.* 2014). Increased temperature, rising sea levels, altered precipitation patterns, and changes in snow cover are all indicators of climate change (Ayalew *et al.* 2022). These changes are largely caused by the emission of greenhouse gases including carbon dioxide (CO₂), methane (CH₄), and nitrous oxide (N₂O), which are linked to the usage of fossil fuels (IPCC 2014a, 2014b). In most cases, greenhouse gas emissions increase surface temperatures, which alter evapotranspiration and precipitation (Bates *et al.* 2008). According to several studies, hydrological systems are extremely susceptible to climatic changes (IPCC 2007; Bates *et al.* 2008; Zereini & Hötzl 2008; Toulmin 2009; Niang *et al.* 2014). Changes in temperature and precipitation affect catchment ecosystems, which in turn affect water availability and increase the frequency of hydrological extremes such as drought and floods (Rotich & Mulungu 2017; Shagega *et al.* 2019; Awotwi *et al.* 2021; Gurara *et al.* 2021).

Several studies have reported a decreasing rainfall trend in many parts of the Sub-Saharan region over the past years (Niang *et al.* 2014). Also, the near-surface temperature in the region has risen by more than 0.5 °C over the last 50 years (IPCC 2007). In contrast to the maximum temperature, the minimum temperature has risen more rapidly (Niang *et al.* 2014). According to Niang *et al.* (2014), the mean annual temperature across the majority of the sub-Saharan region is predicted to rise by 2 °C in the middle of the twenty-first century, and by 4 °C in the late twenty-first century, under the representative concentration pathway (RCP)8.5. Similarly, Almazroui *et al.* (2020) predict an increase of the mean temperature by 1.2, 1.5, and 1.8 °C under weak (SSP1-2.6), moderate (SSP2-4.5), and strong (SSP5-8.5) forcing, respectively. Additionally, persistent droughts and floods are predicted in areas bordering the western Indian Ocean, including most parts of eastern Africa (IPCC 2007).

In Tanzania, climate change and its impacts on catchments hydrology have been the subjects of interest in recent years (Gulacha & Mulungu 2017; Luhunga *et al.* 2018; Shagega *et al.* 2018; Ayugi *et al.* 2021). A study by Gulacha & Mulungu (2017) in the Wami-Ruvu basin reported a change of precipitation by -68 to 328% and -56 to 199% during the 2050s, under SRES A2 and B2 scenarios, respectively, with respect to the baseline period of 1961–1990. The study further reports a change of 0.2 – 7.5 °C and -0.4 to 1.5 °C from the 2020s to the 2080s for maximum and minimum temperature, respectively. Similarly, Näschen *et al.* (2019) in the Kilombero catchment predicted an increase in temperature, and rainfall change of approximately -8.3 to 22.5% in the 2060s, under RCP4.5 and RCP8.5. Also, a streamflow change of 61.6 – 67.8% was predicted. Another study by Shagega *et al.* (2019) in the Ngerengere River catchment predicted an increase of temperature between 0.2 and 2.6 °C in the 2050s, and between 2.7 and 4.4 °C in the 2080s, under the SRES A2 scenario, but the rainfall was predicted to decrease by 3 – 58% . According to these studies, changes in temperature and precipitation will have a considerable impact on the hydrology of catchments. However, because the majority of studies were carried out at the regional level, they are less helpful for planning and managing water resource infrastructures at the catchment scale (IPCC 2014b). This is partially due to the region's diverse climate, which varies from one catchment to another (Mbungu 2016). Therefore, climate prediction needs to be made at a finer spatial scale in order to provide reliable results (Toulmin 2009). In addition, past studies have paid less attention to the high-humidity tropical region where the Upper Ruvu River watershed (URRW) is located. This region is unique due to high rainfall variability resulting from Intertropical Convergence Zone and El Nino-Southern Oscillation (Mbungu 2016). As a result, the prediction of future climatic conditions and their effects on streamflows is critical for water resource planners and watershed stakeholders to enable effective water resource management.

Furthermore, global circulation models (GCMs) have been the widely used tools for the prediction of future meteorological conditions around the globe (Eisner *et al.* 2017; Wang *et al.* 2018; Ahmed *et al.* 2019; Givati *et al.* 2019). Most frequently, hydrologic models rely on the output of the downscaled GCMs to predict future hydrologic conditions (Chen *et al.* 2012). For climate projections in eastern Africa, particularly Tanzania, it has been a common practice for researchers to use a single GCM (Shagega *et al.* 2018). However, studies indicate that the amount of uncertainty associated with a single GCM prediction is fairly high (Wang *et al.* 2018; Ahmed *et al.* 2019), hence multi-model ensembles are strongly recommended in order to reduce these uncertainties (Deb *et al.* 2018). In this context, integrating data from multiple GCM outputs is particularly desired in order to generate reliable estimates (Rotich & Mulungu 2017; Deb *et al.* 2018).

Therefore, the main objective of this study is to assess the impacts of climate change on streamflows in the high-humid tropical URRW. The specific objectives are: (1) generating future climate scenarios in the URRW based on multiple GCMs under RCP4.5 and RCP8.5; (2) developing, calibrating, and validating the Hydrologic Engineering Center's Hydrologic Modeling System (HEC-HMS) model to represent the catchment hydrology; and (3) quantifying the potential impacts of climate change on the streamflows of the URRW.

Study area

This study focuses on the URRW of the Wami-Ruvu basin in Tanzania (Figure 1(a)). The watershed is found on the hinterland of the east African coast between $6^{\circ}40'$ – $7^{\circ}45'S$ and $37^{\circ}15'$ and $38^{\circ}30'E$, with a total area of about $7,663$ km². The watershed elevation ranges from 43 to $2,630$ msl. It is dominated by slopes ranging from 0 to 4.4% , which occupy about 56.1% of the catchment area (Figure 1(b)). Approximately 21.7% of the watershed area is occupied by slopes ranging from 4.4 to 22.8% , and the remaining area has slopes ranging from 22.8 to 187.7% (Figure 1(b)). Higher slopes are found along the Uluguru mountainous area, which essentially increase the rate of soil erosion and deposition along the Kidunda flood plains. The watershed has a diverse topography and consequently varying drainage characteristics throughout the area. The important geographical features in the watershed are the Uluguru Mountains which are part of the Eastern Arc Mountains with elevations extending to $2,630$ msl.

The watershed is mainly characterized by the Rhodic Ferrasols which are found on the extreme west and in the middle part of the sub-catchment (Figure 2(b)). Other soil types are Umbric Acrisols, Mollic Fluvisols, Ferralic Cambisols, and Haplic Acrisols. A small part around Kidunda downstream is covered by Haplic Lixisols, Eutric Vertisols, Eutric Planosols, and Eutric Fluvisols (Figure 2(b)). Most of the watershed area consists of forest reserves and Uluguru mountainous area, which to a large extent remain undisturbed. However, the land cover (approximately 5.2%) along the Mgeta flood plain has been slightly changed in recent years due to the growing population (Figure 2(a)).

The mean annual rainfall is about $1,164$ mm, whereby the mountainous area receives considerably higher rainfall compared to the remaining area. The main rainfall season is March to May, and the dry period usually occurs from June to

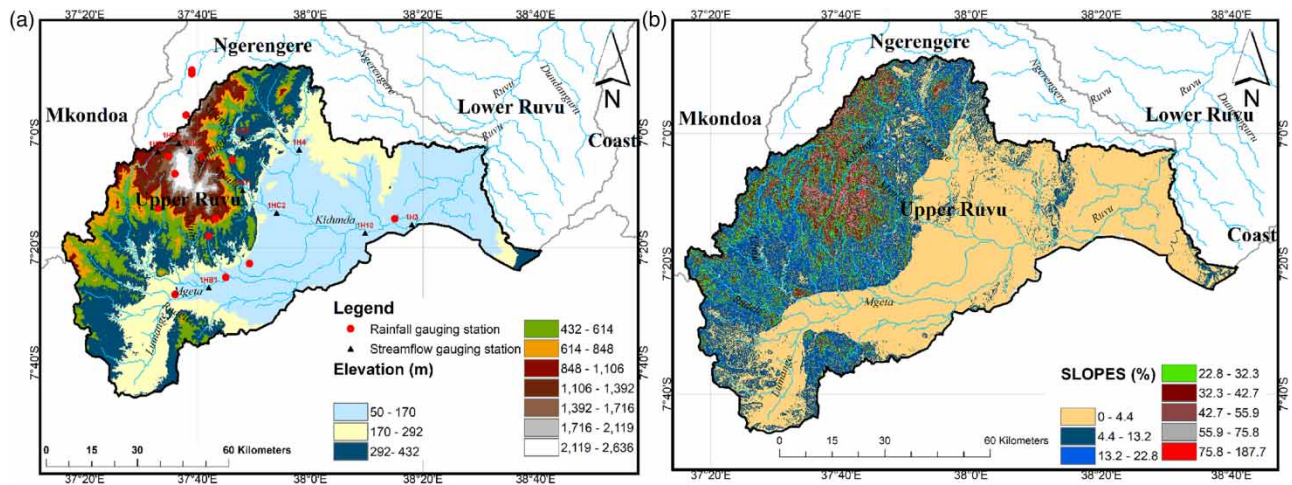


Figure 1 | The map of the URRW showing (a) topography and hydro-meteorological stations and (b) slopes.

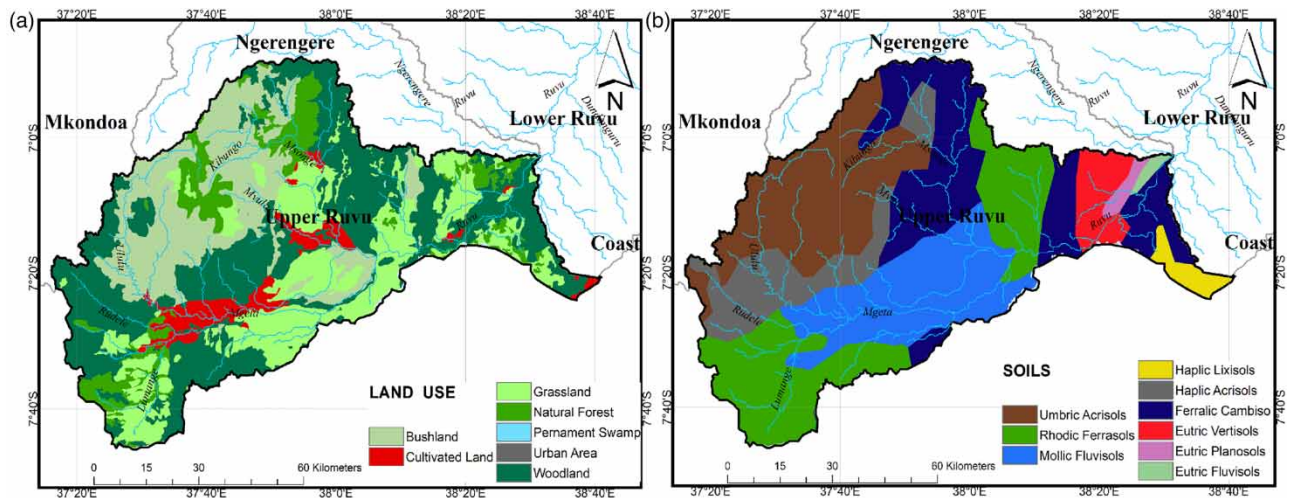


Figure 2 | The map of the URRW showing (a) land use/land cover and (b) soil types.

October (Figure 3(a)). The mean annual minimum and maximum temperatures are 21.3 and 32.1 °C, respectively. The mean monthly maximum temperature is usually higher in January, February, March, November, and December, while the lowest mean monthly maximum temperature usually occurs in July, August, and September. The minimum temperature was found to follow the same trend as the maximum temperature. The relative humidity ranges from 68 to 82% which is classified as high according to Ku-Mahamud & Khor (2009). The peak streamflow ranges from 49.8 to 74.8 m³/s, which is usually observed between April and May, while minimum streamflow ranges from 6.2 to 11.19 m³/s, and is usually observed between September and January (Figure 3(b)). The mean daily streamflow is approximately 46 m³/s.

Data

The digital elevation model (DEM), hydro-meteorological, and land use/cover data were used for developing, calibration, and validation of the HEC-HMS model for this study. The observed climatic data were used for calibration and validation of LARS-WG, while the projected temperature and rainfall data for RCP4.5 and RCP8.5 were used for generating the future streamflows. In this study, the hydro-meteorological data for the baseline period (1951–1978) were obtained from the Wami-Ruvu Water Basin office, which has daily records for 11 rainfall stations (Table 1), 2 climatic stations, and 10 streamflow stations. For the calibration of the hydrologic model, one streamflow station (1H10) was used. The selected streamflow

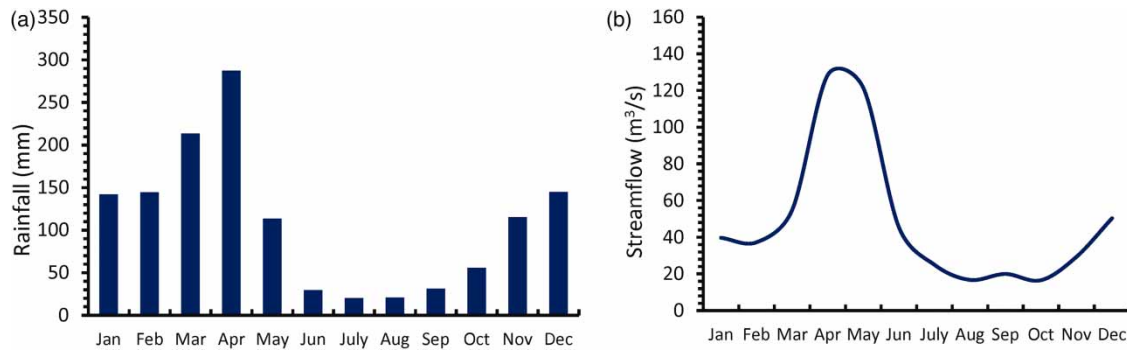


Figure 3 | The plots of (a) mean monthly rainfall and (b) the mean monthly streamflow of the study area.

Table 1 | A summary of meteorological stations used in this study

S/N	Station ID	Station name	Lat	Long	Alt	Rainfall	Temperature
1.	09737006	Matombo Mission	-7.08	37.77	388	x	
2.	09738016	Mikula	-7.25	38.25	84	x	x
3.	09637045	Mondo	-6.95	37.63	1,285	x	
4.	09637052	Morogoro Hydromet	-6.82	37.65	512	x	
5.	09737000	Duthumi Estate	-7.38	37.82	91	x	
6.	09737024	Kibungo Mission	-7.07	37.68	975	x	
7.	09737015	Bunduki	-7.03	37.62	1,281	x	
8.	09737008	Kisaki	-7.47	37.60	183	x	
9.	09737011	Kikeo Mission	-7.22	37.55	610	x	
10.	09737016	Mizungu Mgeta	-7.07	37.58	1,097	x	
11.	09637076	Morogoro Met.	-6.82	37.65	512		x
12.	09737013	Chenzema Mission	-7.12	37.60	1,676	x	

gauging station has relatively complete streamflow records and represents a significant area of the watershed. The daily outputs of rainfall and maximum and minimum temperatures from six CMIP5 GCMs under RCP4.5 and RCP8.5 (Table 2) were extracted from World Climate Research Programme (WCRP) website (<https://esgf-node.llnl.gov/search/cmip5/>). Moreover, the Space Shuttle Radar Topographical Mission (SRTM) DEM with 30 m spatial resolution was downloaded from USGS Earth Explorer. The land use/cover data were also downloaded from USGS Earth explorer and processed by using

Table 2 | A summary of selected GCMs for this study

S/N	Model	Resolution	Institution
1.	ACCESS1-3	1.25° × 1.25°	Commonwealth Scientific and Industrial Research Organization/Bureau of Meteorology, Australia
2.	Bcc-csm1-1	2.8° × 2.8°	Beijing Climate Center, China Meteorological Administration, China
3.	CanESM2	2.8° × 2.8°	Canada Centre for Climate Modelling and Analysis, Canada
4.	IPSL-CM5A-MR	2.5° × 1.25°	Institut Pierre Simon Laplace, France
5.	HadGEM2-ES	1.875° × 1.25°	Met Office Hadley Centre, UK
6.	MIROC5	1.4° × 1.4°	Atmosphere and ocean research institute (the University of Tokyo), National Institute for Environmental Studies, and Japan Agency for Marine-Earth Science and Technology

ArcGIS software. The processed land use/cover maps were further verified by using site surveys, existing maps from the Tanzania Ministry of Water, and satellite imagery. The soil data for the study area were obtained from the International Soil Reference & Information Center (ISRIC) database and were verified using locally available maps.

METHODS

The hydrometric and meteorological data were first checked for missing data and consistency which would otherwise cause biases in the study results (Ayalew *et al.* 2022). The data consistency was checked by the double mass curve method. In addition, a number of common techniques for filling in missing data including the inverse distance weighting, normal ratio, and multiple linear regression methods were considered and analysed in this study. The normal ratio method was found to provide relatively accurate estimates and therefore was adopted for filling in missing rainfall data. Filling of missing data was only applied at the Mondo rainfall station which had a significant length of missing values. Also, the change point analysis was conducted in order to establish the baseline period for this study. The abrupt changes were analysed by using Pettit's, Buishand's, Hubert Segmentation, and Bayesian method of Lee and Heghinian tests (Rougé *et al.* 2013). These tests were carried out by using the Khronostat software developed by the French Institute of Research for Development (IRD).

The climate projections were carried out by using the outputs of six CMIP5 GCMs (Table 2) under RCP4.5 and RCP8.5. The RCP4.5 scenario was chosen because it represents the on-going global collaborative effort to reduce the consequences of climate change, whereas the RCP8.5 scenario was chosen because it represents the highest radiative forcing among the four RCPs (Moss *et al.* 2008). Both scenarios are widely used by water resources planners for developing mitigation and adaptation strategies owing to climate change impacts (Niang *et al.* 2014). The CMIP5 GCMs were first ranked based on their spatial resolution, and then we selected the commonly used GCMs in the tropical region that has a finer spatial resolution. The generation of climate scenarios was carried out by using LARS-WG. The HEC-HMS model was then developed, calibrated, and validated by using the observed hydro-meteorological data. The HEC-HMS model performance was evaluated by using Nash–Sutcliffe efficiency (NSE) and the coefficient of determination (R^2), as described in Table 3. The LARS-WG generated climate scenarios were combined to generate the ensemble-mean (EM) climate scenario, which was then incorporated into a calibrated HEC-HMS model for simulating the future streamflow in the watershed.

Calibration and validation of LARS-WG

The GCMs outputs are usually at a coarse spatial scale; hence, downscaling is commonly applied (Ma *et al.* 2021). The downscaling techniques are usually divided into two categories, namely statistical and dynamic, the former was used in this study. The Long Ashton Research Station Weather Generator (LARS-WG) was employed for downscaling the GCM outputs and generation of climate scenarios. The LARS is a stochastic weather generator commonly used for downscaling GCMs at a single site (Chisanga *et al.* 2017). It is a series-based weather generator that employs semi-empirical distributions for generating wet and dry series, solar radiation, minimum and maximum temperatures, as well as daily precipitation (Chisanga *et al.* 2017). LARS-WG employs a site-specific semi-empirical distribution with 23 intervals to estimate the probability distribution of dry and wet series of daily rainfall as well as minimum and maximum temperatures (Hassan *et al.* 2013). In LARS-WG, a

Table 3 | A mathematical description and interpretation (according to Moriasi *et al.* 2007) of statistical criteria used for evaluating HEC-HMS model performance

	NSE	R^2
Mathematical equation	$1 - \frac{\sum_{i=1}^n (Q_{s(i)} - Q_{o(i)})^2}{\sum_{i=1}^n (Q_{o(i)} - \overline{Q_{oi(l)}})^2}$	$\left(\frac{\sum_{i=1}^n (Q_{o(i)} - \overline{Q_{oi(l)}})(Q_{s(i)} - \overline{Q_{si(l)}})}{\sqrt{\sum_{i=1}^n (Q_{o(i)} - \overline{Q_{oi(l)}})^2 * \sum_{i=1}^n (Q_{s(i)} - \overline{Q_{si(l)}})^2}} \right)^2$
Performance measures		
Very good	>0.75	> 0.85
Good	0.65 < NSE ≤ 0.75	0.75 < R^2 ≤ 0.85
Satisfactory	0.5 < NSE ≤ 0.65	0.60 < R^2 ≤ 0.75

Note. Q_o and Q_s are observed and simulated streamflow values, respectively. ‘-’ on the top of the variable denotes the mean value.

value of a climatic variable (Z_i) corresponding to the probability (P_i) is determined by using Equation (1).

$$Z_i = \min \{Z: P(Z_{\text{obs}} \leq Z) \geq P_i\}, \quad i = 0, 1, 2, 3, \dots, n \quad (1)$$

where P is the probability based on observed data $\{Z_{\text{obs}}\}$.

For each climatic variable, P_0 and P_n are set to 0 and 1, respectively, with corresponding values of $Z_0 = \min \{Z_{\text{obs}}\}$ and $Z_n = \max \{Z_{\text{obs}}\}$. The downscaling process begins with the selection of a random value from one of the intervals, followed by the selection of a random value by using the uniform distribution (Hassan *et al.* 2013). In order to correctly assess the climatic variables, P_i is assigned close to 1 for extremely high values and close to 0 for extremely low values. The remaining intervals are evenly distributed in the probability scale (Chisanga *et al.* 2017).

In this study, the observed rainfall, and minimum and maximum temperatures data were used for the calibration of the LARS-WG. The performance of LARS-WG was validated by using Kolmogorov–Smirnov (K–S) test as well as t and F -tests to compare means, standard deviations, and probability distributions. These tests search for differences between the simulated and observed data. Each test calculates a p -value which is used to determine whether the simulated and observed data have the same distribution. A very low p -value (below 0.01) indicates that the observed and simulated values are unlikely to have the same distribution, hence poor model performance (Chisanga *et al.* 2017). Additionally, the simulated versus observed values of mean monthly rainfall, daily rainfall maxima, minimum daily minima and maxima, and maximum daily minima and maxima were also used to assess the goodness of fit. The calibrated LARS-WG was then used to generate the synthetic data of rainfall and the maximum and minimum temperatures for two periods (2041–2060 (the 2050s) as near future and 2081–2100 (the 2080s) as far future) under RCP4.5 and RCP8.5.

Calibration and validation of the HEC-HMS model

The HEC-HMS is a conceptual semi-distributed hydrologic model widely used for event-based and continuous modelling (Halwatura & Najim 2013). The model is widely used in tropical regions and has proven to provide reliable simulations (Gumindoga *et al.* 2017). Due to data quality and scarcity, the model was calibrated by using 5-year records (1969–1974) and validated by using 4-year records (1975–1978), at a 1H10 streamflow gauging station. The HEC-HMS model inputs data were the daily values of rainfall, the estimates of evapotranspiration, streamflow, and DEM. The estimates of evapotranspiration were computed from minimum and maximum temperature values by using the FAO ETo Calculator version 3.2. During the calibration of the HEC-HMS model, the simplex method was employed for the optimization of model parameters. The soil moisture accounting (SMA) was used as the loss method, and baseflow contribution was computed by the linear reservoir (LR) method. In SMA, the volume of the infiltration is computed according to Equation (2), the percolation between the upper soil and groundwater (GW) layer is computed according to Equation (3) and the GW contribution is calculated according to Equation (4). The model performance was evaluated by using the statistical indices (NSE and R^2 ; Table 3), and the comparison of simulated and observed hydrographs.

$$\text{Psi} = \text{MaxSi} - \left(\frac{\text{CSs}}{\text{MaxSs}} \right) \times \text{MaxSi} \quad (2)$$

where Psi is the potential soil infiltration, MaxSi is the maximum soil infiltration, CSs is the current volume of soil storage, and MaxSs is the maximum volume of the soil storage.

$$\text{PSP} = \text{MaxSp} \times \left(\frac{\text{CSs}}{\text{MaxSs}} \right) \left(\frac{1 - \text{CGWs}}{\text{MaxGWs}} \right) \quad (3)$$

where PSP is the potential soil percolation rate, MaxSp is the maximum percolation rate, CGWs is the calculated layer 1 groundwater storage, MaxGWs is the maximum storage for layer 1 groundwater storage.

$$\text{GW}_{t+1} = \frac{\text{PSP} + \text{CGWs} + \text{PGWp} + 0.5\text{GW}_t \times \text{ts}}{\text{RGWs} + 0.5\text{ts}} \quad (4)$$

where GW_t is the groundwater flow at a current time step, GW_{t+1} is the groundwater flow at the next time step, PGWp is the potential ground water percolation, ts is the time step, and RGW is the routing coefficient for groundwater storage.

Sensitivity analysis is an important aspect of hydrological modelling (Song *et al.* 2015). It is used to rank model parameters according to their impacts on model output and helps in identifying the optimal parameters during model calibration (Pechlivanidis *et al.* 2011). The sensitivity analysis for the HEC-HMS model was performed manually by changing one parameter at a time as described by Ayalew (2019). The value of the model parameter was increased and decreased by 40% at a 5% interval while observing the value of NSE. In this study, a total of 17 HEC-HMS model parameters were subjected to sensitivity analysis.

RESULTS AND DISCUSSION

Calibration and validation of the LARS-WG

The change point analysis for meteorological data (1951–1978) was done at the annual time scale using a 0.05 significant level. The results indicated no significant break in the distribution of the annual rainfall series; hence, the baseline period (1951–1978) was selected based on the available data.

The results of the K–S test, t -test, and F -test indicated that the LARS-WG was able to simulate well the seasonal distribution of wet and dry periods (Table 4), monthly rainfall (Table 5), as well as minimum and maximum temperatures (Table 5). The plots of simulated and observed mean monthly rainfall also indicated a good correlation with an R^2 of 0.99. The simulated

Table 4 | The results of the K–S test for seasonal wet/dry SERIES distribution

Season	Wet/dry	N	K-S	p -Value	Performance
DJF	Wet	11.5	0.003	1.000	Perfect fit
DJF	Dry	11.5	0.075	1.000	Perfect fit
MAM	Wet	11.5	0.115	0.996	Very good fit
MAM	Dry	11.5	0.061	1.000	Perfect fit
JJA	Wet	11.5	0.032	1.000	Perfect fit
JJA	Dry	11.5	0.058	1.000	Perfect fit
SON	Wet	11.5	0.163	0.892	Very good fit
SON	Dry	11.5	0.095	1.000	Perfect fit

Table 5 | The results of the K–S test for daily rainfall and minimum and maximum temperature distributions

Month	N	Daily rain		Daily T_{min}		Daily T_{max}	
		K-S	p -Value	K-S	p -Value	K-S	p -Value
Jan	12	0.065	1.000	0.053	1.000	0.053	1.000
Feb	12	0.195	0.726	0.053	1.000	0.053	1.000
Mar	12	0.065	1.000	0.053	1.000	0.106	0.999
Apr	12	0.065	1.000	0.053	1.000	0.033	1.000
May	12	0.067	1.000	0.105	0.999	0.000	1.000
Jun	12	0.137	0.972	0.053	1.000	0.053	1.000
Jul	12	0.124	0.990	0.053	1.000	0.053	1.000
Aug	12	0.1	1.000	0.053	1.000	0.053	1.000
Sep	12	0.08	1.000	0.053	1.000	0.053	1.000
Oct	12	0.065	1.000	0.053	1.000	0.106	0.999
Nov	12	0.112	0.997	0.053	1.000	0.053	1.000
Dec	12	0.064	1.000	0.053	1.000	0.053	1.000

monthly minimum and maximum temperatures and daily maxima were also compared with observed values and yielded an R^2 of 0.99 (Figure 4). These results indicate that the LARS-WG can be reliably used for projecting the rainfall, as well as maximum and minimum temperatures in the URRW.

Calibration and validation of the HEC-HMS model

The sensitivity analysis for 18 HEC-HMS model parameters was performed, and the SMA parameters were found to be more sensitive (Figure 5). Among the SMA parameters, surface imperviousness was found to be the most sensitive, followed by the GW coefficient. However, soil percolation and storage parameters were found to be less sensitive (Figure 5). The statistical indices indicate that the HEC-HMS model performed well in both calibration and validation periods. The model yielded the NSE and R^2 of 0.76 and 0.76, respectively, during calibration, and NSE and R^2 of 0.68 and 0.76, respectively, during validation. The model performance is rated very good according to Moriasi *et al.* (2007). Moreover, the observed and simulated hydrographs shown in Figure 6 indicated that the model simulated well the pattern of observed hydrographs, as well as low and moderate flows. However, there was a slight difference between observed and simulated peak flows, whereby 22% underestimation and 4% overestimation were indicated during calibration and validation periods, respectively. This could be associated with the model structural deficiencies; however, a number of studies in neighbouring watersheds, including Shagega *et al.* (2019) in the Ngerengere catchment and Wambura *et al.* (2015) in the Wami sub-basin, have reported similar challenges for HBV and SWAT models, respectively. As a result, inaccurate peak flow estimation could also be linked to

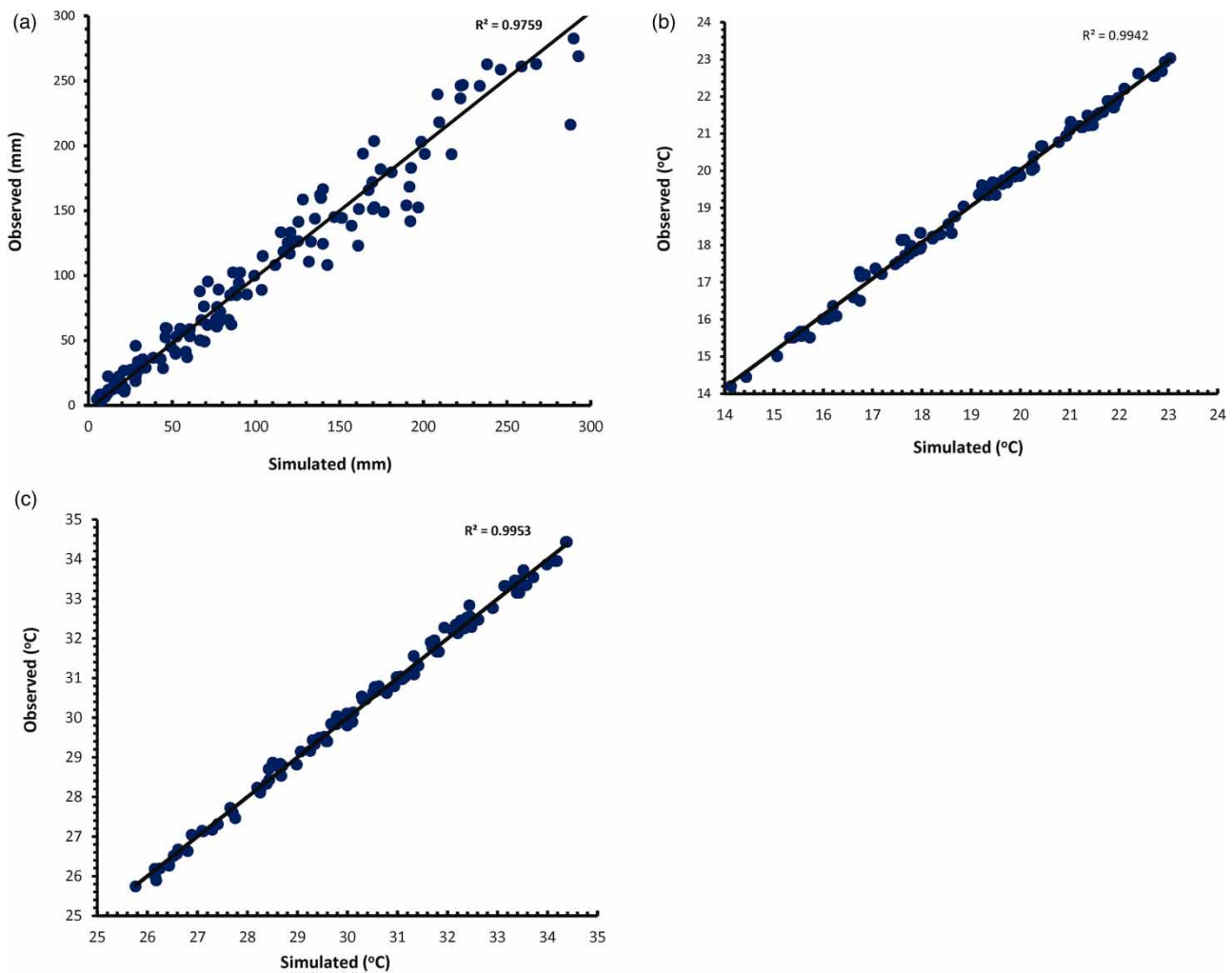


Figure 4 | The scatter plots of LARS-WG-simulated and observed: (a) mean monthly rainfall; (b) minimum temperature; and (c) maximum temperature in the URRW.

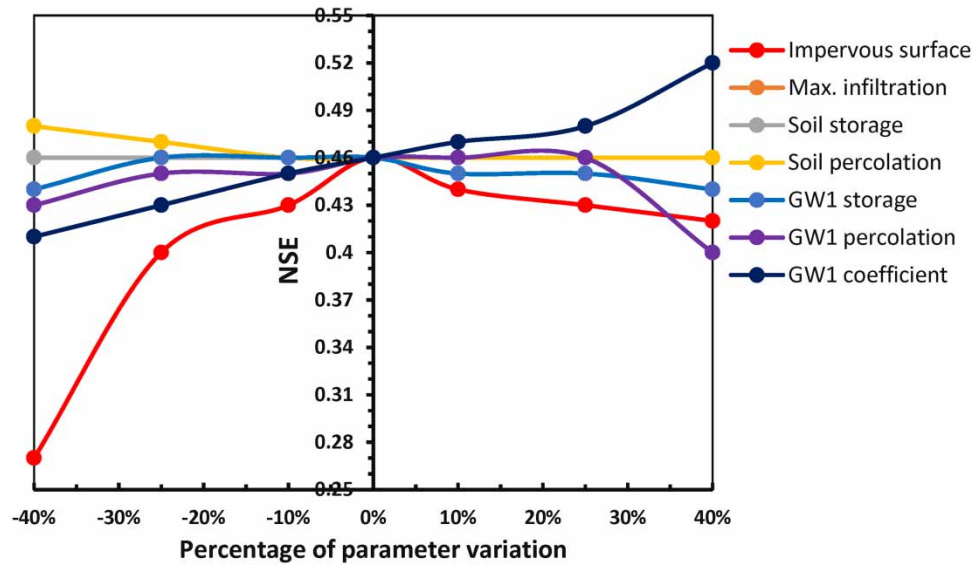


Figure 5 | The plot of sensitivity analysis of HEC-HMS model parameters.

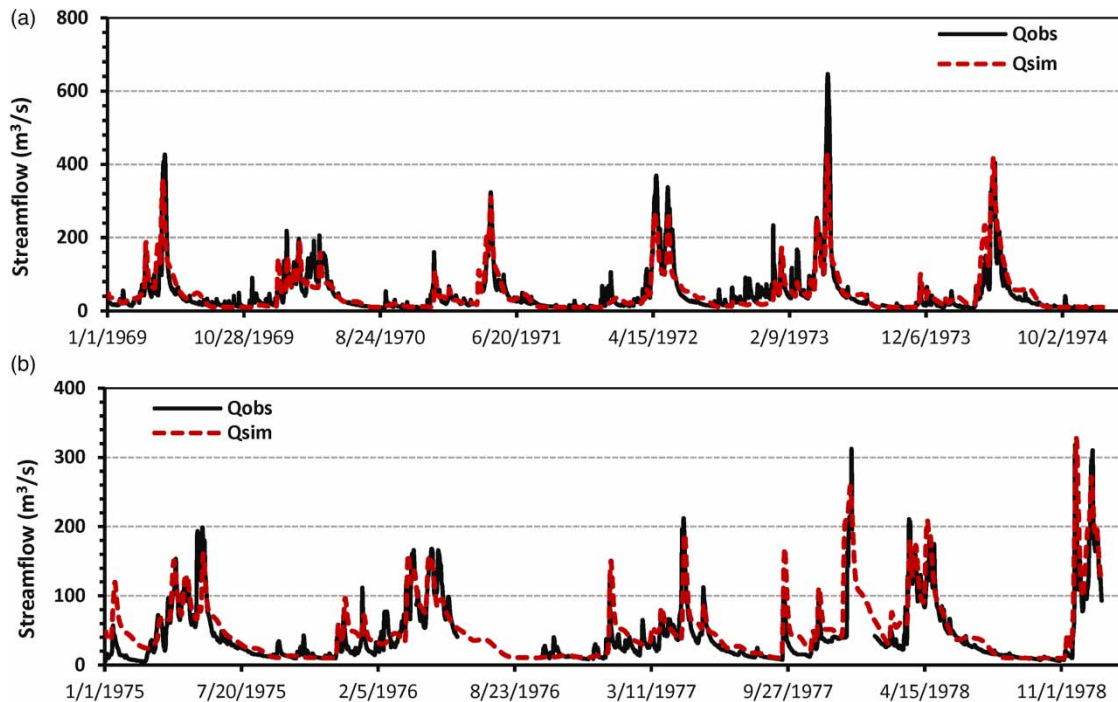


Figure 6 | The observed and HEC-HMS-simulated streamflow during (a) calibration and (b) validation.

the scarcity of streamflow data, in which the observed peaks are not sufficient enough to be adequately simulated. However, the statistical evaluation indicates that the HEC-HMS model can be reliably used for simulating the streamflow in the watershed.

Projected changes in meteorological conditions

An analysis of mean monthly rainfall indicates an increase of 2.9–76.4% under RCP4.5 and 6.7–78% under RCP8.5 in the 2050s, while an increase of 10–80% under RCP4.5, and 8–68% under RCP8.5 is predicted in the 2080s (Figure 7). During

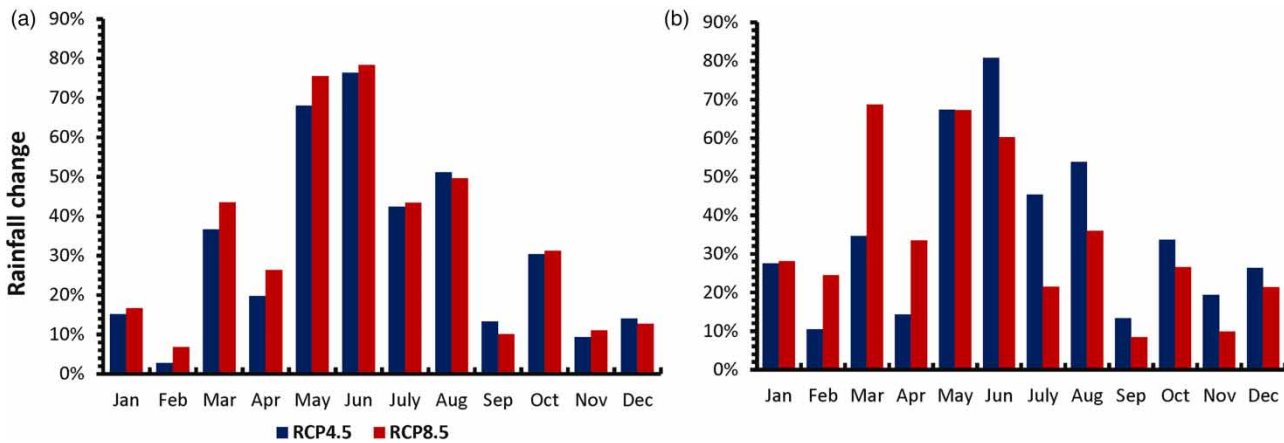


Figure 7 | The projected monthly rainfall changes in (a) the 2050s and (b) the 2080s periods, under RCP4.5 and RCP8.5 scenarios.

the 2050s, a significant increase in the mean monthly rainfall will potentially occur in May (68%), June (76%), and August (51%) under RCP4.5, while an increase of 75, 78, and 50% is predicted for May, June, and August, respectively, under RCP8.5. Similarly, a significant increase in the mean monthly rainfall will potentially occur in May, June, and August during the 2080s, under both RCP4.5 and RCP8.5. Also, a significant increase in mean monthly rainfall is predicted for March under RCP8.5. The mean annual rainfall is also expected to increase in most stations for both periods, except Bunduki, where a small decrease is predicted under both scenarios, as shown in Figure 8.

The minimum temperature is predicted to increase by -0.43 to 0.56 °C under RCP4.5 and 0.07 – 1.02 °C under RCP8.5 in the 2050s (Figure 9). During the 2080s, the minimum temperature is predicted to increase by 0.16 – 3.1 °C under both scenarios (Figure 9). Overall, the minimum temperature shows an average change of -0.05 and 0.45 °C during the 2050s, and 0.53 and 2.7 °C during the 2080s under RCP4.5 and RCP8.5, respectively. On the other hand, the change in maximum temperature is predicted to range between -0.74 and 0.83 °C, and -0.05 and 1.22 °C under RCP4.5, during the 2050s and 2080s, respectively, whereas the change of -0.26 to 1.28 and 1.79 – 3.0 °C is predicted during the 2050s and 2080s, respectively, under RCP8.5. In general, the average change of maximum temperature under RCP4.5 and RCP8.5 is predicted to be -0.007 and 0.41 °C in the 2050s, and 0.47 and 2.4 °C in the 2080s, respectively. From these results, it can be clearly seen that both maximum and minimum temperatures will change dramatically under RCP8.5. This, in turn, is expected to increase evapotranspiration rates, leading to a decrease in streamflow. When relating the change of monthly rainfall, temperature, and

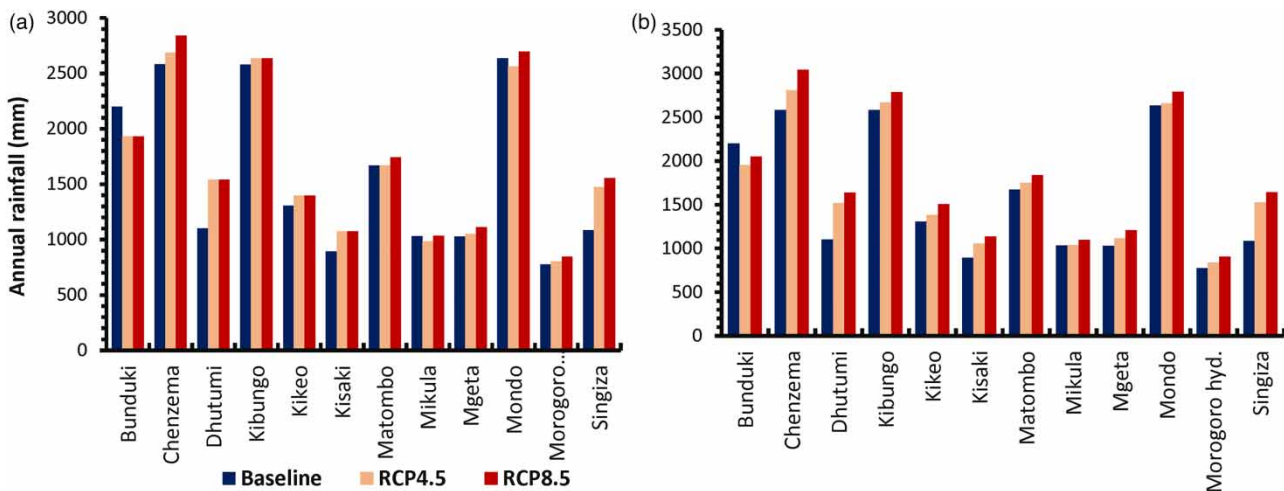


Figure 8 | The baseline and projected annual rainfall at various stations during (a) the 2050s and (b) the 2080s, under RCP4.5 and RCP8.5 scenarios.

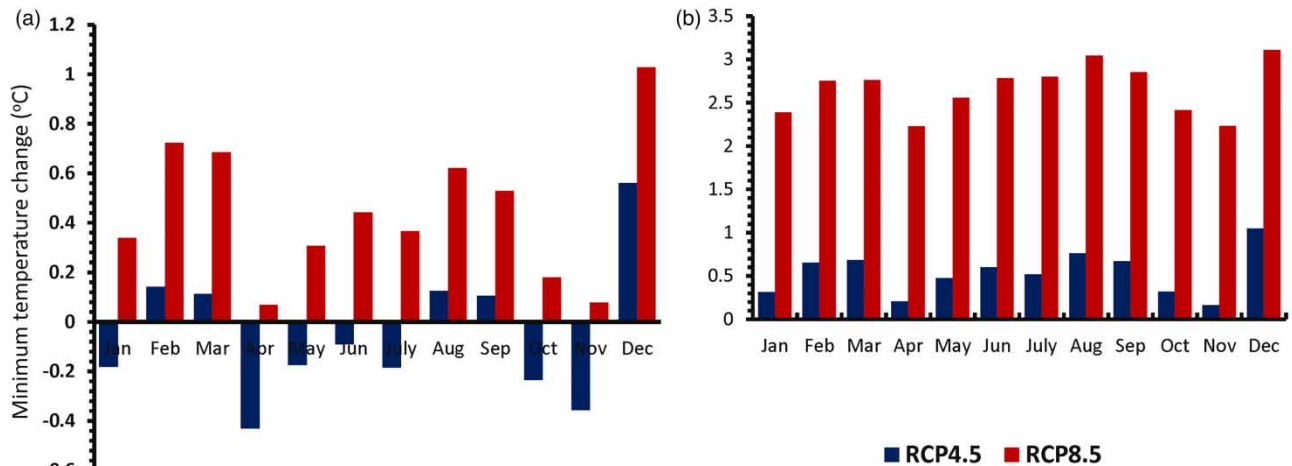


Figure 9 | The projected monthly changes of minimum temperature in (a) the 2050s and (b) the 2080s, under RCP4.5 and RCP8.5 scenarios.

streamflows (Figures 7, Figures 9–11), it can be clearly seen that the temperature will have significant impacts especially in months with lower rainfall.

To gain more insight into projected future meteorological conditions in the region, the results of this study were compared with a number of studies from neighbouring catchments. The study results were found to be consistent with Shagega *et al.* (2018) in the Ngerengere catchment which projected an increase in rainfall, and minimum and maximum temperatures in the 2050s and 2080s under the SRES A2 scenario. Similarity is also found in several studies in the region (Gulacha & Mulungu 2017; Kishiwa *et al.* 2018; Näschen *et al.* 2019). Consistency in projections essentially reduces uncertainties, allowing for more efficient planning and management of water resource infrastructures.

Analysis of future streamflow changes

An increase in streamflow is predicted from March to August in both the 2050s and 2080s, but the decrease will potentially occur in the remaining months (Figures 11 and 12). In general, the average change of streamflow is projected to be -10.72 and 0.36% in the 2050s, and -2.83 and 16.42% in the 2080s, under RCP4.5 and RCP8.5, respectively. As shown in Figures 11 and 12, the streamflow will decrease in January and February, as well as from September to December, in both periods, under both scenarios. The projected streamflow from September to February months is against the projected mean monthly rainfall

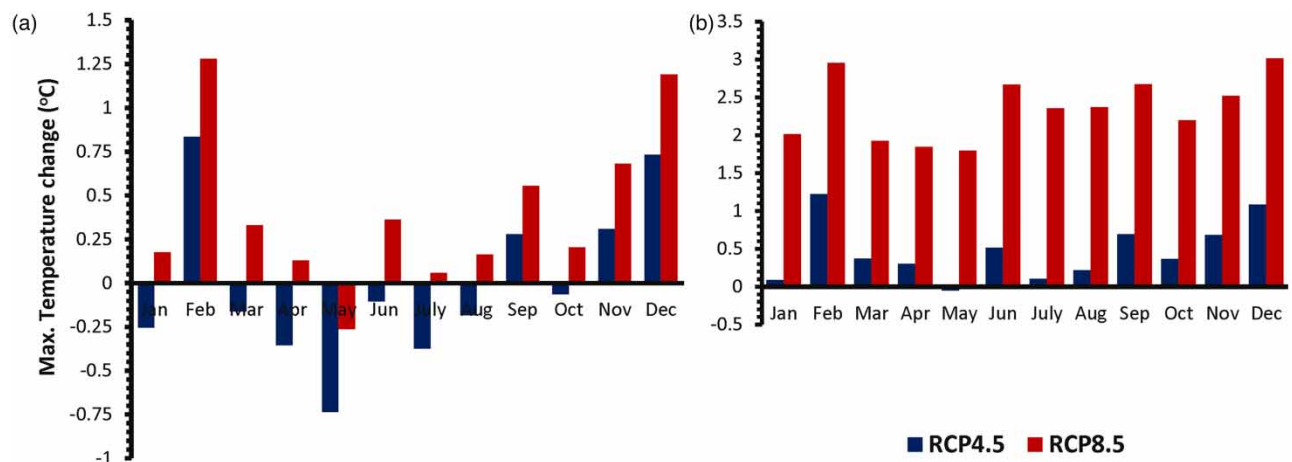


Figure 10 | The projected changes of monthly maximum temperature in (a) the 2050s and (b) the 2080s, under RCP4.5 and RCP8.5 scenarios.

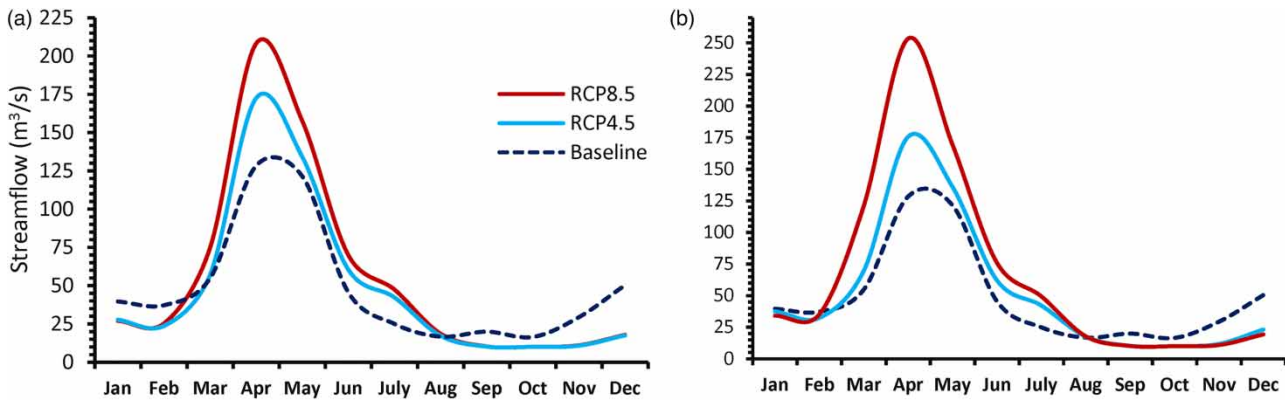


Figure 11 | The plots of baseline and projected streamflow hydrograph during (a) the 2050s and (b) the 2080s, under RCP4.5 and RCP8.5 scenarios.

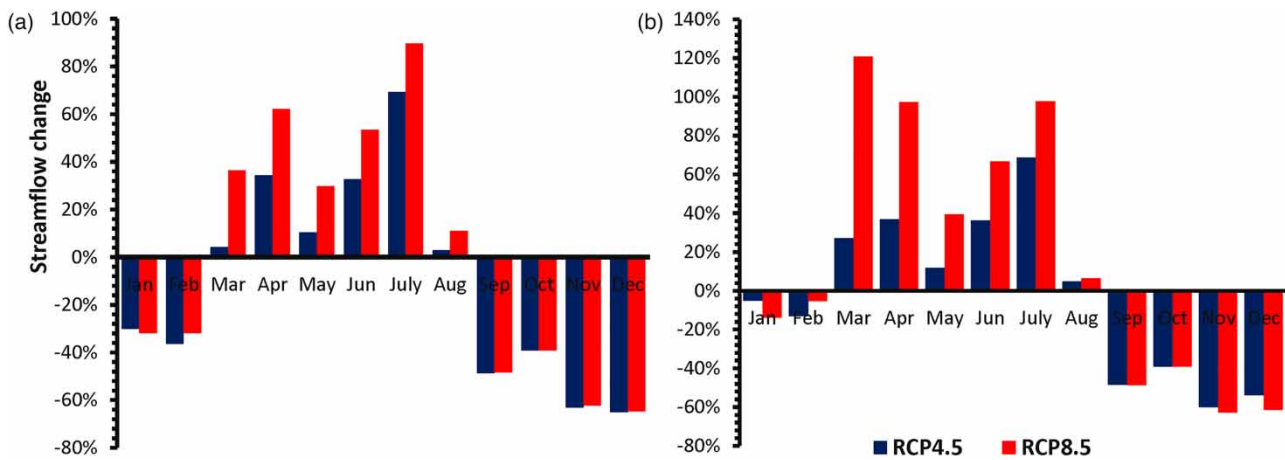


Figure 12 | The plots of percentage change of month streamflow in (a) the 2050s and (b) the 2080s, under RCP4.5 and RCP8.5 scenarios.

(Figure 7), which is expected to rise in these months for both the periods, under RCP4.5 and RCP8.5. As previously stated, this aligns with positive temperature changes that will potentially increase the evapotranspiration rates. Also, an analysis of minimum streamflow indicates that there will be a positive change from January to August, but a negative change is predicted from September to December in the 2050s, under RCP4.5 and RCP8.5 (Figure 13). In the 2080s, however, positive changes in minimum streamflow are projected from January to August and November, and December, while negative

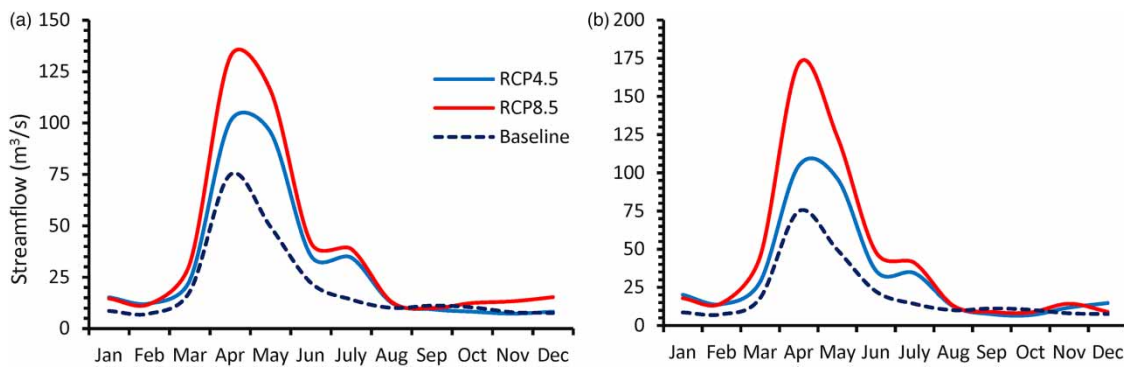


Figure 13 | The plots showing the change of monthly minimum flows in (a) the 2050s and (b) the 2080s, under RCP4.5 and RCP8.5 scenarios.

changes are only projected from September to October. On the other hand, the maximum streamflow shows a negative change in all months except for June and July under RCP8.5, in the 2050s (Figure 14). Also, a positive change of maximum streamflow is projected for June and July under RCP4.5, but no change is indicated in March, April, and May. However, significant differences are indicated in the 2080 s, whereby maximum flows are projected to be higher from April to August, and lower in the remaining months under RCP8.5. In addition, the maximum flows are expected to be lower in all months except in July under RCP4.5.

The flow duration curves are useful when assessing the streamflow indices that are widely used by planners in planning, designing, and managing water resources infrastructures. In most cases, the low flows (less than Q_{70}), medium flows (Q_{20} – Q_{70}), and high flows (greater than Q_{20}) are usually used (Saez *et al.* 2018), hence they have been analysed in this study (Figure 15). The results indicate that high flows will be significantly higher in the 2050s and 2080s under both scenarios. For comparison, the value of Q_5 is predicted to be 273 and 315 m^3/s in the 2050s, and 200 and 276 m^3/s under RCP4.5 and RCP8.5, respectively, while the Q_5 for the baseline period is 143 m^3/s . This is equivalent to a 90 and 120% increase in the 2050s, and a 40 and 93% increase in the 2080s under RCP4.5 and RCP8.5, respectively. Also, the medium flows are generally expected to be higher except for Q_{50} – Q_{70} and Q_{65} – Q_{70} , which are predicted to be slightly lower in 2050s and 2080s, respectively. For comparison, the projected Q_{50} in the 2050s are 25 and 26 m^3/s , and 31 and 31.5 m^3/s in the 2080s, under RCP4.5 and RCP8.5, respectively, whereas the Q_{50} for the baseline period is 26.6 m^3/s . This is equivalent to a decrease of approximately 6 and 2% in the 2050s, and an increase of 17 and 18% in

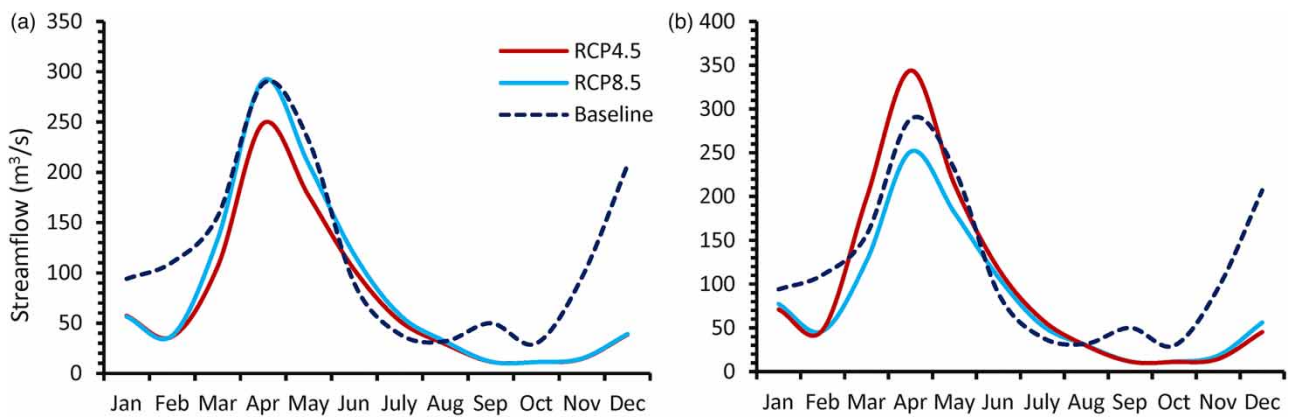


Figure 14 | The plots showing the change of monthly maximum flows during (a) the 2050s and (b) the 2080s, under RCP4.5 and RCP8.5 scenarios.

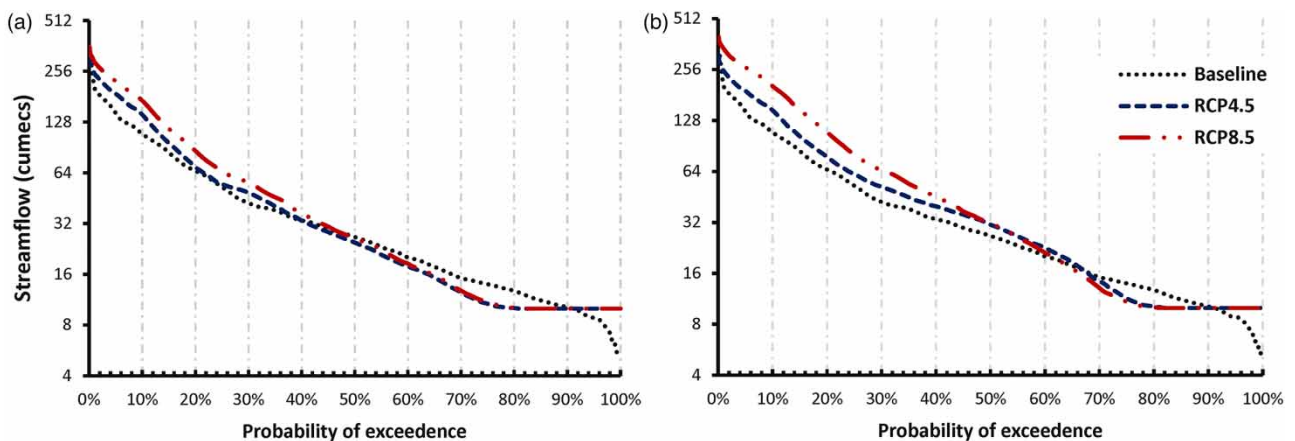


Figure 15 | The FDCs for baseline and projected streamflow during (a) the 2050s and (b) the 2080s, under RCP4.5 and RCP8.5 scenarios.

the 2080s. Moreover, the low flows (Q_{70} – Q_{90}) are projected to be lower in both periods, but very low flows (less than Q_{90}) are projected to be higher. For comparison, the Q_{75} for the baseline period is $13.7 \text{ m}^3/\text{s}$, while the projected Q_{75} are 10.7 and $10.9 \text{ m}^3/\text{s}$ during the 2050s, and 11.1 and $10.6 \text{ m}^3/\text{s}$ during the 2080s under RCP4.5 and RCP8.5, respectively. On the other hand, the Q_{95} for the baseline period is $8.6 \text{ m}^3/\text{s}$, while the projected Q_{95} in both periods is $10 \text{ m}^3/\text{s}$, under both scenarios.

Conclusions and recommendations

In this study, the impacts of climate change on streamflow in the URRW were evaluated. First, the meteorological data were analysed for abrupt changes in order to establish the baseline period. The Khronostat software was used for analysing the abrupt changes in the observed rainfall distributions. The results indicated that there was no break in meteorological data. As a result, 1951–1978 was selected as the baseline period. The climate projections were made from six CMIP5 GCMs outputs, which were then downscaled by the calibrated LARS-WG at each station. The EM scenario was then computed and incorporated into the calibrated and validated HEC-HMS model for future streamflow projections.

The LARS-WG was found to be a reliable tool for generating climate scenarios for the URRW. The rainfall and minimum and maximum temperatures were well simulated with R^2 above 0.726 for all variables. Moreover, the daily streamflow observed at the 1H10 streamflow station was used for calibration and validation of the HEC-HMS model. The calibration and validation results indicated that the HEC-HMS model is suitable for the streamflow simulation in the watershed. The model yielded the NSE and R^2 of 0.76 and 0.76 during calibration, and 0.68 and 0.76 during validation, respectively. This performance is good considering the data scarcity in the watershed.

Furthermore, the EM scenario derived from multiple GCMs was used for projecting the watershed streamflows. This approach is well described by [Ma et al. \(2021\)](#) and provides reliable estimates since direct averaging of the GCMs outputs smooths the climatic variability. The findings indicate that future climate changes will have significant meteorological impacts on the streamflow of the URRW. It was found that the monthly rainfall could potentially increase by 6.7–78% during the 2050s, while an increase of 8–80% is predicted during the 2080s, under RCP4.5 and RCP8.5. The minimum temperature could potentially change between -0.43 and $1.02 \text{ }^\circ\text{C}$ during the 2050s, and 0.16 and $3.1 \text{ }^\circ\text{C}$ during the 2080s, while the maximum temperature could potentially change between -0.74 and $1.28 \text{ }^\circ\text{C}$ during the 2050s, and -0.05 and $3.0 \text{ }^\circ\text{C}$ during the 2080s, under RCP4.5 and RCP8.5.

The meteorological changes will have impacts on streamflow which is anticipated to change by -65.1 to 89.7% during the 2050s, and -62.9 to 120.9% during the 2080s, under RCP4.5 and RCP8.5. On a monthly scale, a decrease in streamflow is projected for January (30%), February (36%), September (49%), October (39%), November (63%), and December (65%) months, while the increase in streamflow is projected in March (4.2%), April (34%), May (10%), June (33%), July (69%), and August (3%) months. Additionally, a comparison of baseline and projected minimum and maximum streamflow revealed significant changes. The results indicate that a significant minimum streamflow change of approximately 20 – $41 \text{ m}^3/\text{s}$ during the 2050s, and 22 – $97 \text{ m}^3/\text{s}$ during the 2080s could potentially occur in April under RCP4.5 and RCP8.5. Maximum streamflow is also expected to change significantly in April for both periods. Moreover, a comparison of flow duration curves (FDCs) indicates an overall increase of high flows (larger than Q_{20}), very low flows (smaller than Q_{95}), and moderate flows (between Q_{20} and Q_{70}) under both scenarios. However, the low flows (between Q_{70} and Q_{90}) will be slightly lower.

The results of this study are based on six GCMs and only two scenarios (RCP4.5 and RCP8.5). As described by [Ma et al. \(2021\)](#), incorporating more GCMs and emission scenarios for hydrological studies is important for a better understanding of associated uncertainties. Therefore, it is recommended to incorporate additional GCMs and emission scenarios in order to generalize the study findings. Moreover, the HEC-HMS model was calibrated and validated by using 5- and 4-year streamflow data, respectively. Although the model was able to simulate well the watershed streamflow, it is recommended to recalibrate the model once the new data are available.

Additionally, the impacts of future land use/cover change were not incorporated in this study. Despite the fact that the majority of the watershed area is currently undisturbed, changes in land use/cover are expected to be significant in the near future due to the growing population in the watershed. Therefore, streamflow projections in future studies should consider both climate and use/cover changes in order to increase the accuracy of the results.

Overall, the results of this study are important for providing an insight into the future climate conditions and surface water availability on URRW. However, they should be used with care by considering the study limitations. Also, this study is a starting point for future studies in URRW and other high-humid tropical catchments.

ACKNOWLEDGEMENT

We acknowledge the support offered by the Department of Water Resources Engineering of the University of Dar es salaam during data collection.

AUTHOR CONTRIBUTIONS

N.T. conceptualized, investigated, did data curation, performed the methodology, did formal analysis, visualized, and wrote the original draft. D.M.M.M. conceptualized, investigated, validated, supervised, wrote, reviewed, and edited the article. F.I. investigated, validated, supervised, wrote, reviewed and edited the article.

DATA AVAILABILITY STATEMENT

Data cannot be made publicly available; readers should contact the corresponding author for details.

CONFLICT OF INTEREST

The authors declare there is no conflict.

REFERENCES

- Ahmed, K., Sachindra, D. A., Shahid, S., Demirel, M. C. & Chung, E. S. 2019 Selection of multi-model ensemble of general circulation models for the simulation of precipitation and maximum and minimum temperature based on spatial assessment metrics. *Hydrology and Earth System Sciences* **23** (11), 4803–4824.
- Almazroui, M., Saeed, F., Saeed, S., Islam, M. N. & Ismail, M. 2020 Projected change in temperature and precipitation over Africa from CMIP6. *Earth Systems and Environment* **4** (3), 455–475.
- Awotwi, A., Annor, T., Anornu, G. K., Quaye-Ballard, J. A., Agyekum, J., Ampadu, B., Nti, I. K., Gyampo, M. A. & Boakye, E. 2021 Climate change impact on streamflow in a tropical basin of Ghana, West Africa. *Journal of Hydrology: Regional Studies* **34**, 341–325.
- Ayalew, A. T. 2019 Rainfall-runoff modeling: a comparative analysis: semi distributed HBV light and SWAT models in Geba catchment, Upper Tekeze Basin, Ethiopia. *American Journal of Science, Engineering and Technology* **4** (2), 34–40.
- Ayalew, D. W., Asefa, T., Moges, M. A. & Leyew, S. M. 2022 Evaluating the potential impact of climate change on the hydrology of Ribb catchment, Lake Tana Basin, Ethiopia. *Journal of Water and Climate Change* **13** (1), 190–205.
- Ayugi, B., Dike, V., Ngoma, H., Babaousmail, H., Mumo, R. & Ongoma, V. 2021 Future changes in precipitation extremes over east Africa based on CMIP6 models. *Water* **13** (17), 1–19.
- Bates, B., Kundzewicz, Z. W., Wu, S. & Palutukof, J. 2008 *Climate Change and Water. Technical Paper of the Intergovernmental Panel on Climate Change*. Intergovernmental Panel on Climate Change, Geneva.
- Chen, H., Xu, C. & Guo, S. 2012 Comparison and evaluation of multiple GCMs, statistical downscaling and hydrological models in the study of climate change impacts on runoff. *Journal of Hydrology* **434**, 36–45.
- Chisanga, C. B., Phiri, E. & Chinene, V. R. N. 2017 Statistical downscaling of precipitation and temperature using long Ashton research station weather generator in Zambia: a case of mount Makalu agriculture research station. *American Journal of Climate Change* **06** (03), 487–512.
- Deb, P., Babel, M. S. & Francis, A. 2018 Multi-GCMs approach for assessing climate change impact on water resources in Thailand. *Modeling Earth Systems and Environment* **4**, 181–115.
- Eisner, S., Flörke, M., Chamorro, A., Daggupati, P., Donnelly, C., Huang, J., Hundecha, Y., Koch, H., Kalugin, A., Krylenko, I., Mishra, V., Piniewski, M., Samaniego, L., Seidou, O., Wallner, M. & Krysanova, V. 2017 An ensemble analysis of climate change impacts on streamflow seasonality across 11 large river basins an ensemble analysis of climate change impacts on streamflow seasonality across 11 large river basins. *Climatic Change* **141**, 161–118.
- Givati, A., Thirel, G., Rosenfeld, D. & Paz, D. 2019 Climate change impacts on streamflow at the upper Jordan River based on an ensemble of regional climate models. *Journal of Hydrology: Regional Studies* **21**, 2192–2109.
- Gulacha, M. M. & Mulungu, D. M. M. 2017 Generation of climate change scenarios for precipitation and temperature at local scales using SDSM in Wami-Ruvu River Basin, Tanzania. *Physics and Chemistry of the Earth, Parts A/B/C* **100**, 1062–1072.

- Gumindoga, W., Rwasoka, D. T., Nhapi, I. & Dube, T. 2017 [Ungauged runoff simulation in upper Manyame catchment, Zimbabwe: application of the HEC-HMS model](#). *Physics and Chemistry of the Earth* **100** (2), 371–382.
- Gurara, M. A., Jilo, N. B. & Tolche, A. D. 2021 Modelling climate change impact on the streamflow in the Upper Wabe Bridge watershed in Wabe Shebele River Basin, Ethiopia. *International Journal of River Basin Management* **19**, 101–113.
- Halwatura, D. & Najim, M. M. M. 2013 Application of the HEC-HMS model for runoff simulation in a tropical catchment. *Environmental Modelling and Software* **46**, 46155–46162.
- Hassan, Z., Shamsudin, S. & Harun, S. 2013 Application of SDSM and LARS-WG for simulating and downscaling of rainfall and temperature. *Theoretical and Applied Climatology* **116**, 114243–114257.
- IPCC 2007 *Climate Change 2007: Impacts, Adaptation and Vulnerability. Contributions of Working Group II to the Fourth Assessment Report of the Intergovernmental Panel on Climate Change*. Cambridge University Press, Cambridge, United Kingdom and New York, NY, USA.
- IPCC 2014a *Climate Change 2014: Impacts, Adaptation, and Vulnerability. Part A: Global and Sectoral Aspects. Contribution of Working Group II to the Fifth Assessment Report of the Intergovernmental Panel on Climate Change*. Cambridge University Press, Cambridge, United Kingdom and New York, NY, USA.
- IPCC 2014b *Climate Change 2014: Impacts, Adaptation, and Vulnerability. Part B: Regional Aspects. Contribution of Working Group II to the Fifth Assessment Report of the Intergovernmental Panel on Climate Change*. Cambridge University Press, Cambridge, United Kingdom and New York, NY, USA.
- Kishiwa, P., Nobert, J., Kongo, V. & Ndomba, P. 2018 Assessment of impacts of climate change on surface water availability using coupled SWAT and WEAP models: case of upper Pangani River Basin, Tanzania. *Proceedings of the International Association of Hydrological Sciences* **378**, 37823–37827.
- Ku-Mahamud, K. R. & Khor, J. Y. 2009 [Pattern extraction and rule generation of forest fire using sliding window technique](#). *Computer and Information Science* **2** (3), 113–121.
- Luhunga, P. M., Kijazi, A. L., Chang, L. & Kondowe, A. 2018 Climate change projections for Tanzania based on high-resolution regional climate models from the coordinated regional climate downscaling experiment. *Frontiers in Environmental Science* **6** (122), 1–20.
- Ma, D., Gu, H. & Sun, Z. 2021 Assessing climate change impacts on streamflow and sediment load in the upstream of the Mekong River basin. *Climatology* **41**, 413391–413410.
- Mbungu, W. B. 2016 *Impacts of Land Use and Land Cover Changes, and Climate Variability on Hydrology and Soil Erosion in the Upper Ruvu Watershed, Tanzania*. Virginia State University.
- Moriasi, D. N., Arnold, J. G., Liew, M. W. V., Bingner, R. L., Harmel, R. D. & Veith, T. L. 2007 Model evaluation guidelines for systematic quantification of accuracy in watershed simulations. *American Society of Agricultural and Biological Engineers* **50** (3), 885–900.
- Moss, R., Babiker, M., Brinkman, S., Eduardo, C., Carter, T., Edmonds, J., Ismail, E., Seita, E., Lin, E., Kathy, H., Roger, J., Mikiko, K., Kelleher, J., Francois, J., Manning, M., Matthews, B., Meehl, J., Meyer, L. & Mitchell, J. 2008 *Towards New Scenarios for Analysis of Emissions, Climate Change, Impacts, and Response Strategies*. Intergovernmental Panel on Climate Change (IPCC), Geneva.
- Näschen, K., Diekkrüger, B., Leemhuis, C. & Seregina, L. S. 2019 Impact of climate change on water resources in the Kilombero Catchment in Tanzania. *Water* **11** (859), 1–28.
- Niang, I., Ruppel, O., Abdrabo, M., Essel, A., Lennard, C., Padgham, J. & Urquhart, P. 2014 *Africa. In: Climate Change 2014: Impacts, Adaptation, and Vulnerability. Part B: Regional Aspects. Contribution of Working Group II to the Fifth Assessment Report of the Intergovernmental Panel on Climate Change*. Cambridge University Press, United Kindom and New York, NY, USA.
- Pechlivanidis, I. G., Jackson, B. M., Mcintyre, N. R. & Wheeler, H. S. 2011 Catchment scale hydrological modelling: a review of model types, calibration approaches and uncertainty analysis methods in the context of recent developments in technology and applications. *Global Nest Journal* **13** (3), 193–214.
- Rotich, S. C. & Mulungu, D. M. M. 2017 [Adaptation to climate change impacts on crop water requirements in Kikafu catchment, Tanzania](#). *Journal of Water and Climate Change* **02** (08), 274–292.
- Rougé, C., Ge, Y. & Cai, X. 2013 Detecting gradual and abrupt changes in hydrological records. *Advances in Water Resources Journal* **53**, 5333–5344.
- Saez, J. P., Aparicio, J. S., Sancez, J. P. & Velazquez, D. P. 2018 A comparison of SWAT and ANN models for daily runoff simulation in different climatic zones of Peninsular Spain. *Water* **10** (192), 1–19.
- Shagega, F. P., Munishi, S. E. & Kongo, V. 2018 Prediction of future climate in Ngerengere river catchment, Tanzania. *Physics and Chemistry of the Earth* **112**, 112200–112209.
- Shagega, F. P., Munishi, S. E. & Kongo, V. M. 2019 Assessment of potential impacts of climate change on water resources in Ngerengere catchment, Tanzania. *Physics and Chemistry of the Earth* **3** (18), 1–19.
- Song, X., Zhang, J., Zhan, C., Xuan, Y., Ye, M. & Xu, C. 2015 [Global sensitivity analysis in hydrological modeling: review of concepts, methods, theoretical framework, and applications](#). *Journal of Hydrology* **523** (225), 739–757.
- Toulmin, C. 2009 *Climate Change in Africa*. Zed Books and IAI, London and New York.
- Wambura, J. F., Ndomba, M. P., Kongo, V. & Tumbo, D. S. 2015 Uncertainty of runoff projections under changing climate in Wami River sub-basin. *Journal of Hydrology: Regional Studies* **4**, 4333–4348.

- Wang, B., Zheng, L., Liu, D. L., Ji, F., Clark, A. & Yu, Q. 2018 Using multi-model ensembles of CMIP5 global climate models to reproduce observed monthly rainfall and temperature with machine learning methods in Australia. *International Journal of Climatology* **38** (13), 4891–4902.
- Zereini, F. & Hötzl, H. 2008 *Climatic Changes and Water Resources in the Middle East and North Africa*. Springer International Publishing, Berlin.

First received 24 May 2022; accepted in revised form 17 August 2022. Available online 30 August 2022